Journal of Coastal Research	10	3	600–620	Fort Lauderdale, Florida	Summer 1994

Historical Shoreline Mapping (II): Application of the Digital Shoreline Mapping and Analysis Systems (DSMS/DSAS) to Shoreline Change Mapping in Puerto Rico

E. Robert Thieler† and William W. Danforth‡

†Duke University
Department of Geology
Program for the Study of Developed Shorelines
Campus Box 90228
Durham, NC 27708, U.S.A.

‡U.S. Geological Survey[1]
Branch of Atlantic Marine Geology
Quissett Campus
Woods Hole, MA 02543, U.S.A.

ABSTRACT

THIELER, E.R. and DANFORTH, W.W., 1994. Historical shoreline mapping (II): Application of the Digital Shoreline Mapping and Analysis Systems (DSMS/DSAS) to shoreline change mapping in Puerto Rico. *Journal of Coastal Research*, 10(3), 600-620. Fort Lauderdale (Florida), ISSN 0749-0208.

A new, state-of-the-art method for mapping historical shorelines from maps and aerial photographs, the Digital Shoreline Mapping System (DSMS), has been developed. The DSMS is a freely available, public domain software package that meets the cartographic and photogrammetric requirements of precise coastal mapping, and provides a means to quantify and analyze different sources of error in the mapping process. The DSMS is also capable of resolving imperfections in aerial photography that commonly are assumed to be nonexistent. The DSMS utilizes commonly available computer hardware and software, and permits the entire shoreline mapping process to be executed rapidly by a single person in a small lab. The DSMS generates output shoreline position data that are compatible with a variety of Geographic Information Systems (GIS).

A second suite of programs, the Digital Shoreline Analysis System (DSAS) has been developed to calculate shoreline rates-of-change from a series of shoreline data residing in a GIS. Four rate-of-change statistics are calculated simultaneously (end-point rate, average of rates, linear regression and jackknife) at a user-specified interval along the shoreline using a measurement baseline approach.

An example of DSMS and DSAS application using historical maps and air photos of Punta Uvero, Puerto Rico provides a basis for assessing the errors associated with the source materials as well as the accuracy of computed shoreline positions and erosion rates. The maps and photos used here represent a common situation in shoreline mapping: marginal-quality source materials. The maps and photos are near the usable upper limit of scale and accuracy, yet the shoreline positions are still accurate ±9.25 m when all sources of error are considered. This level of accuracy yields a resolution of +0.51 m/yr for shoreline rates-of-change in this example, and is sufficient to identify the short-term trend (36 years) of shoreline change in the study area.

ADDITIONAL INDEX WORDS: *Aerial photography, cartography, coastal erosion, geographic information systems, photogrammetry, shoreline change.*

INTRODUCTION

This paper is the second of two in which we discuss principles of historical shoreline mapping and their application. The first paper (THIELER and DANFORTH, 1994, this volume) presents cartographic and photogrammetric techniques that can be used to obtain geographic shoreline data from maps and aerial photographs. This paper presents the application of a new approach to historical shoreline mapping we have developed based on these techniques: the Digital Shoreline Mapping System (DSMS) (DANFORTH and THIELER, 1992b) and the Digital Shoreline Analysis System (DSAS) (DANFORTH and THIELER, 1992a). This paper summarizes the capabilities of the DSMS and DSAS and presents an example of their application to a typical historical shoreline mapping problem using data from Punta Uvero, Puerto Rico.

THE DIGITAL SHORELINE MAPPING AND ANALYSIS SYSTEMS

To integrate the elements of the shoreline mapping process (THIELER and DANFORTH, 1994, this volume) into a complete software package, the Digital Shoreline Mapping System was developed. The DSMS Version 1.0 (DANFORTH and THIELER, 1992b) is a public-domain suite of programs that produces digital shoreline position data

93051 received 6 May 1993; accepted in revision 14 July 1993.

[1] Use of tradenames is for purposes of identification only and does not constitute endorsement by the U.S. Geological Survey.

from historical maps, charts and aerial photographs. The basic goals in the ongoing development of the DSMS are to make shoreline mapping accurate and easy to execute, using a variety of methods that permit its application not only to shoreline mapping, but also to a wide range of cartographic and photogrammetric mapping projects. A second suite of programs, the Digital Shoreline Analysis System, was developed to calculate shoreline rates-of-change from a time series of shoreline data residing in a Geographic Information System (GIS). The important characteristics of the DSMS and the DSAS are listed in Table 1.

The DSMS and the DSAS run on UNIX-based computers and utilize ASCII text files for input and output. The DSMS programs produce shoreline position data files formatted for use in most popular GIS (*e.g.*, Arc/Info, Atlas GIS, MapInfo, *etc.*). The DSMS also includes a point and track (stream) mode digitizing program (*digin*) that produces DSMS-ready ASCII data files from maps and photos. The DSMS programs are written in both the C and FORTRAN programming languages. The DSAS programs are written in the C programming language. The interfaces for the DSMS v1.0 and DSAS v1.0 utilize UNIX C-shell (csh) scripts executed in a command-line environment.

The DSMS was developed on a Digital Equipment Corporation DECstation 3100 running version 4.2 of the Ultrix operating system (the DEC implementation of UNIX). Summagraphics Microgrid (backlit, 122 × 153 cm) and CalComp 9500 Series (112 × 153 cm) digitizing tables with a resolution of 0.025 mm were used in development and testing.

Because DSMS programs use ASCII text files for both input and output, and comply with accepted standards for UNIX I/O, almost any operating system (*e.g.*, MS-DOS, Macintosh, UNIX), GIS (*e.g.*, Arc/Info) or drafting (*e.g.*, AutoCAD) software can be used to generate input data or view and analyze the output. Thus, the DSMS is highly flexible, and can accept data from and produce data for almost any GIS, CAD, or cartographic software. If necessary, the initial data needed for a mapping project can be entered manually using text files created in a word processor or text editor. This is also an important advantage for testing a project design, viewing intermediate results, or adding different types of input data.

For maps and charts, DSMS programs use UNIX cartographic filters developed by EVENDEN (1990, 1991) to transform X-Y digitizer output to geographic coordinates. Over 70 cartographic projections (*e.g.*, Polyconic, Mercator, State Plane), 24 different ellipsoidal constants and several datums are available. These programs can be used to obtain both ground control point data for use in photogrammetric applications, or to generate shoreline position data from a map. The programs also output residual errors from the transformation process to quantify the accuracy of source materials and the digitizer operator.

For aerial photographs, DSMS features include preprocessing to refine digitized image coordinates, simultaneous aerotriangulation for large

Table 1. *Characteristics of the Digital Shoreline Mapping and Analysis Systems.*

DSMS
Distortion correction and user control of various parameters for photogrammetric mapping: 1) correction for film deformation and atmospheric refraction; 2) simultaneous triangulation of large groups of photographs, including photos of different years, camera focal length, *etc.* using a single set of ground control points; 3) control extension (aerotriangulation) for areas with few temporally or spatially stable reference features; 4) differential weight assignments can be made for all input data to reflect its precision; 5) provides utilities to check for bad data at various stages in the mapping process; 6) adjustable to reflect the elevation of the feature being mapped.
Uses commonly available computer hardware and software, including a GIS-independent point and track mode digitizing program.
Input and output are compatible with most Geographic Information Systems (*e.g.*, Arc/Info).
Extensive error propagation analysis and accuracy assessment of map and photo transformations.
Can use a variety of ground control data (*e.g.*, digitized map data; Transit or GPS surveyed positions; geodetic control table data) for photogrammetric mapping.
Can be used for mapping any feature that has a known, relatively uniform elevation, such as wetland boundaries or lake/reservoir shorelines.
Over 70 map projections and 24 reference datums are available for both map and photograph data.
DSAS
Automatic calculation of shoreline rates-of-change at a user-specified interval along the shoreline using four different methods.
Measurements can be made on highly crenulated coasts without creating data gaps where the shoreline orientation changes.
Output rate of change files are compatible with spreadsheet, presentation graphics, statistical analysis or other software (*e.g.*, Excel, Lotus 1-2-3, SPSS).

groups of spatially and temporally overlapping photos, single-ray intersection of digitized photograph (shoreline) coordinates, and extensive facilities for error analysis. The DSMS programs are modular and designed to be run in sequence. The DSMS preprocessing program, *images*, for example, is used to remove film deformation, reduce measured data from a given set of photos to a common reference coordinate system, quantify residual errors in the digitizing process, and format the data for use in later programs.

Both a single-frame space resection and a group aerotriangulation program are available in the DSMS. The single-frame space resection program, *frames*, can be used early in the data reduction process to check for bad data, or to create input data for the General Integrated Analytical Triangulation (*GIANT*) aerotriangulation program (ELASSAL and MALHOTRA, 1987). The *GIANT* program is commonly used by the National Ocean Service (NOS) and the U.S. Geological Survey (USGS) to generate the camera parameters used in stereoplotting equipment for contouring, profiling, compiling maps (*e.g.*, TP-sheets, topographic quadrangles) and making orthophotomaps from air photos. The DSMS also provides a means to use *GIANT* directly, without requiring an initial single-frame space resection. This approach significantly reduces the ground control requirements for each photograph (see discussion in THIELER and DANFORTH, 1993, this volume).

The *GIANT* aerotriangulation program (ELASSAL and MALHOTRA, 1987) originally was developed for the IBM 6250 computer and later rewritten for Digital Equipment Corporation VAX computers. For integration into the DSMS, however, version 1.1 of the program is being modified to run under UNIX. *GIANT* solves for the ground coordinates of image points measured on two or more photographs and the camera position and attitude for each photograph. The program uses an iterative least squares technique, and assumes uncorrelated observations. All observations, including image coordinate measurements, ground control point locations and camera parameters, can be weighted differentially to reflect knowledge of their precision. A ground control point, for example, can have different weight assignments for each component of latitude, longitude and elevation. Alternatively, control having one or more unknown components (*e.g.*, elevation only) can be used. This permits a variety of horizontal, vertical and fully known control of varying accuracy to be used. The program also furnishes a means to describe the potential errors made during digitizing by allowing the user to specify the standard deviation of digitized photo measurements. The capabilities of the *GIANT* program also include: (1) simultaneous triangulation of large groups of photographs, including photos of differing date, scale, camera focal length, *etcetera* using a common set of ground control points; (2) using either space-rectangular (UTM, State Plane) or geographic coordinate systems; (3) correction for atmospheric refraction based on camera position and attitude; and (4) extensive error propagation analysis.

Camera parameters determined by *GIANT* are used to compute the geographic coordinates of the shoreline points digitized in each photograph by a single-ray intersection technique (THIELER and DANFORTH, 1994, this volume) implemented in the DSMS program, *shoreline*. The geographic shoreline coordinates are output as a tab-delimited ASCII file that can be imported into a variety of Geographic Information Systems.

The DSAS (DANFORTH and THIELER, 1992a) was developed to determine historical shoreline rates-of-change using a time series of shoreline data residing in a GIS. The DSAS v1.0 employs a measurement baseline approach to calculate shoreline rates-of-change at a user-specified interval along the shoreline. The DSAS v1.0 simultaneously calculates the four rate-of-change statistics reviewed by DOLAN *et al.* (1991) (endpoint rate, average of rates, linear regression and jackknifing) at a user-specified interval along the shoreline. Like the DSMS, the programs run on UNIX-based computers and ASCII text files are used for both input and output. DSAS output includes tab-delimited ASCII files that can be used in spreadsheet and statistical software for analysis and presentation.

Input data used in the development and testing of the DSMS and DSAS consisted of: (1) NOS T- and TP-sheet shoreline maps printed on stable-base mylar; (2) USGS 7.5-minute topographic quadrangles printed from the original production plates onto stable-base mylar; and (3) color, black and white, and color infrared air photos (transparencies and paper prints). Shoreline position data for the DSMS/DSAS development study were compiled and edited in MapGrafix, an Apple Macintosh-based GIS. Shoreline change maps used for field checking were plotted on a Hewlett-Packard DraftMaster MX pen plotter. Publication-quality maps were created using the MAG-

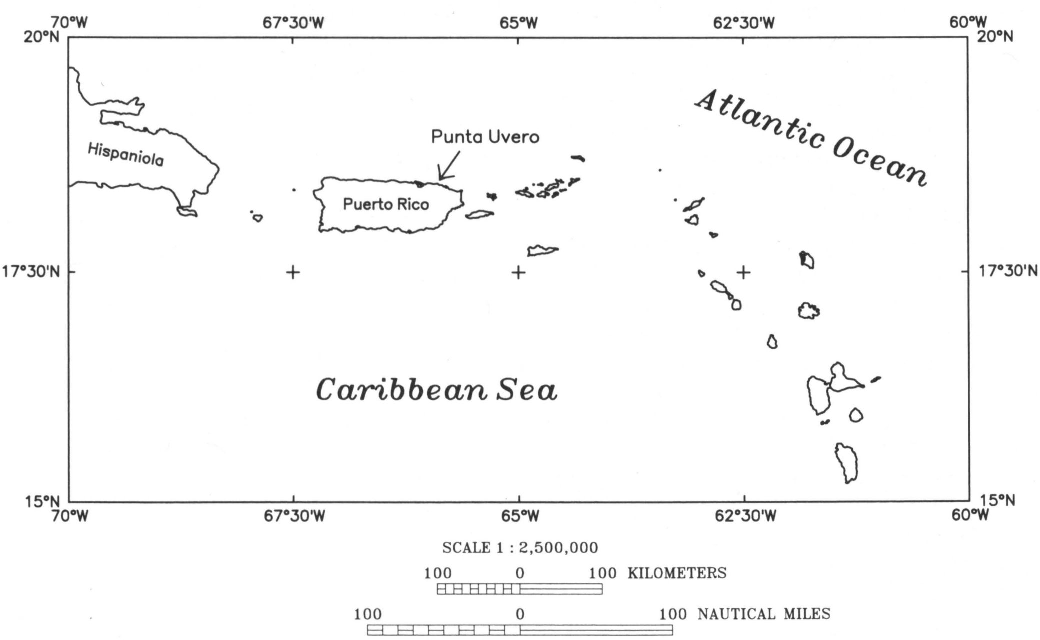

Figure 1. Location map showing Puerto Rico and the Punta Uvero study area on the northeast coast.

PEN (EVENDEN and BOTBOL, 1985) map production package, and plotted on a CalComp 5845 electrostatic plotter.

STUDY AREA

Punta Uvero is part of a low-lying, microtidal (0.3 m) coastal floodplain located about 30 km east of San Juan, Puerto Rico (Figure 1). The shoreline is characterized by an unconsolidated, sandy beach-dune complex (Figure 2). Nearshore reefs located on subaqueous outcrops of Pleistocene eolianite are common (KAYE, 1959).

Changes in the morphology of the coast over time indicate that the once stable sandy shoreline has become highly erosional. Presumably, this has occurred due to the deterioration of the nearshore reefs caused by increased runoff and pollution following the intense development of the area during the 1960's (VELAZCO-DOMÍNGUEZ *et al.*, 1985). The reefs had acted as a natural offshore breakwater, protecting this part of the shoreline from intense wave action. With the natural protection removed, the rate of erosion at Punta Uvero increased dramatically, which led to the construction of seawalls in front of some homes during the mid-1980's (Figure 3).

There are a number of problems associated with historical shoreline mapping in Puerto Rico, because of the limits imposed by the complexity and diversity of the shoreline, as well as the nature of the available data. For example, the 600 km of Puerto Rican coastline contains sandy beaches, rocky headlands, cliffs, alluvial bluffs and mangrove swamps. Other problems include: (1) lack of consistent high-quality air photo coverage, (2) few accurate shoreline maps, (3) limited ground control for use in photogrammetric mapping, (4) available materials are near the usable upper scale limit (1:20,000) for detecting the fairly low rates of shoreline change predominant in Puerto Rico, (5) the highly variable geomorphology of the coast. These conditions are ideal, however, for developing a new mapping technique because they present a wide range of technical situations that

Figure 2. Low altitude oblique photo of Punta Uvero, Puerto Rico taken in 1988. Punta Uvero is located on a low-lying coastal plain about 30 km east of San Juan. The shoreline has been eroding rapidly since the mid-1960's.

Figure 3. The rapid erosion at Punta Uvero prompted the construction of small seawalls in front of some homes. This 1988 photo shows the downdrift erosion caused by the seawall. Historically, this beach was an important recreational resource for bathing and local horse races.

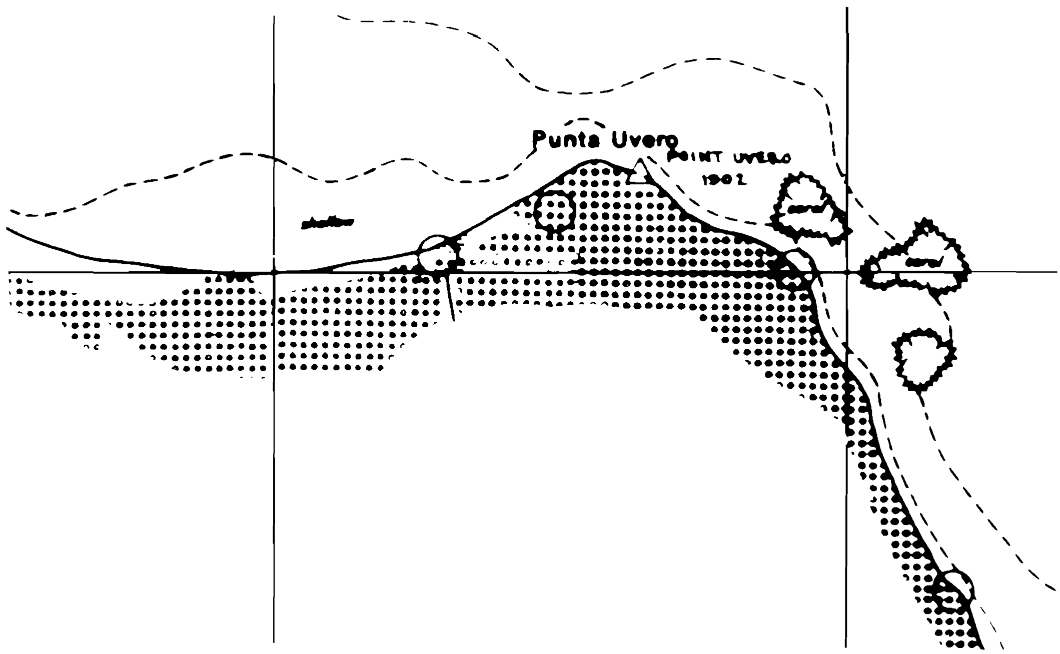

Figure 4. Enlarged section of NOS T-sheet shoreline map T 12136, which was surveyed in 1959. The original map used in this study was printed on stable-base mylar at a scale of 1:10,000.

require a common solution. An additional objective was to develop an efficient method to calculate shoreline rates-of-change for the long stretches of highly crenulated coast common in Puerto Rico.

MATERIALS

Sources of historical data for Puerto Rico include: (1) NOS T- and TP-sheet shoreline maps published between 1901 and 1980 at scales from 1:10,000 to 1:20,000; (2) USGS 7.5-minute topographic quadrangles, published at a scale of 1:20,000; and (3) color and black and white vertical aerial photographs. Several sets of aerial photographs are available for Puerto Rico. The best coverage of the island is provided by aerial surveys performed in 1936, 1951, 1963 and 1987.

Materials used in the example presented here include 1959 and 1964 NOS T-sheets (Figure 4), a USGS 7.5-minute topographic quadrangle (Figure 5), and three sets of air photos taken in 1936, 1951, and 1987 (Figure 6A, 6B and 6C). Each photo set has approximately 10–30 percent overlap between frames.

The maps and photos available for Puerto Rico represent a common situation in shoreline mapping: marginal-quality source materials. The T-sheets, for example, do not cover the entire island, vary highly in quality, and have few well-defined control points that can be used for accuracy tests or as control points in photogrammetric mapping. The best source of ground control data for photogrammetric mapping is supplemental control digitized from USGS topographic 7.5-minute maps, which are generally only accurate to ± 10 m. In addition, nearly all the aerial photography of Puerto Rico has a scale of 1:20,000. The limitations imposed by the source materials are stringent because of their low accuracy relative to the rates of shoreline change that need to be measured. Thus, precise cartographic and photogrammetric techniques are required in order to maximize the potential accuracy of the calculated shoreline positions and shoreline rates-of-change, as well as to quantify inherent errors in the source materials.

METHODS

The DSMS and DSAS programs are designed to be run in sequence. Figure 7 shows the basic steps in DSMS data reduction for maps and pho-

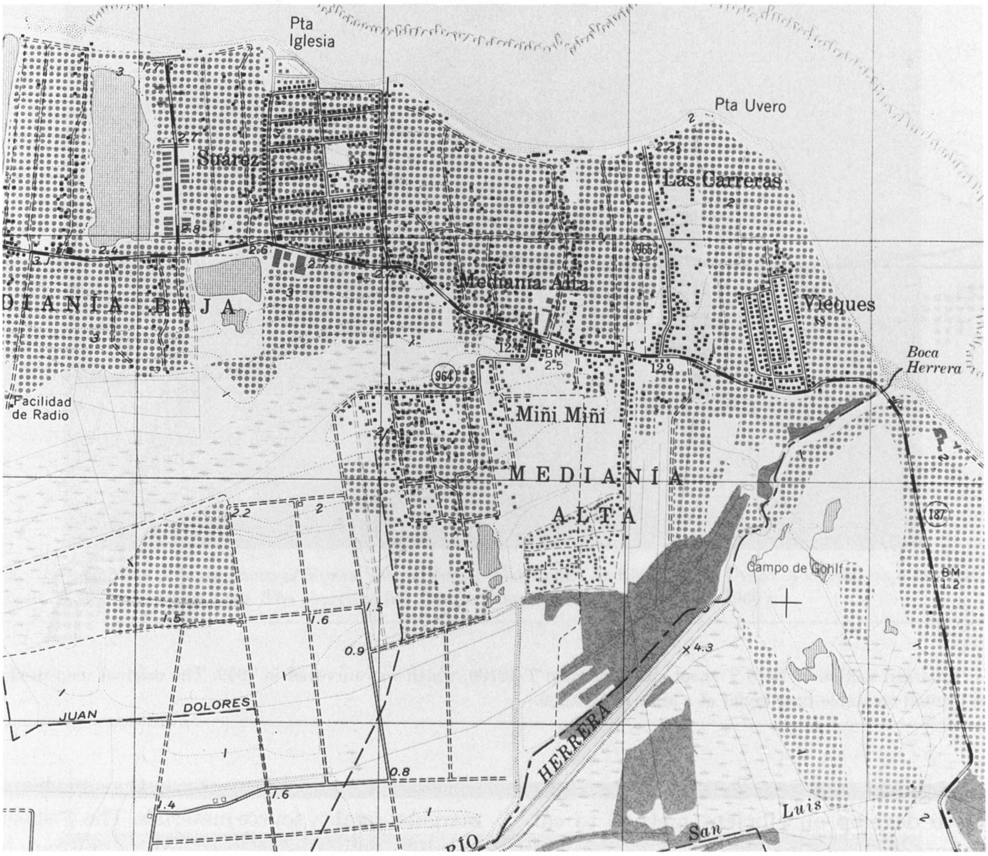

Figure 5. Enlarged section of the USGS 7.5′ quadrangle for Rio Grande, P.R. This 1:20,000 map was printed on mylar and used to obtain ground control point locations for photogrammetric mapping. The map was originally surveyed in 1962 and revised in 1982.

tos used in this study. A complete description of DSMS and DSAS execution is provided by DANFORTH and THIELER (1992a,b). Technical terms not defined here are defined in THIELER and DANFORTH (1994, this volume).

The NOS T-sheet of Punta Uvero has a scale of 1:10,000, and a Polyconic projection based on the Clarke 1866 ellipsoid. The Mean High Water shoreline shown on the T-sheet was digitized using a 5 pts/sec track mode. Eight calibration points (map tick locations) and a first order polynomial transformation were specified in the *mapshore* program to convert the digitizer coordinates to Universal Transverse Mercator (UTM) values based on the Clarke 1866 ellipsoid. The output shoreline coordinate data were then imported into an overlay in a MapGrafix GIS file covering Punta Uvero.

A control network for the air photos was developed using the USGS map, which has a Polyconic projection based on the Clarke 1866 ellipsoid. Ground control points such as buildings, road intersections, and irrigation canals identified on the photos were located on the map, digitized and converted to latitude-longitude and UTM coordinates. The DSMS programs *ground* and *get.ground.points* were used to input the elevation values for each point and format data for use in the space resection and aerotriangulation programs.

The air photos were digitized using a 6 × lighted magnifying loupe to aid in identification of the fiducial reference marks around the photo border, ground control, pass points and the shoreline. For the 1951 and 1987 photos, fiducials in the center of each side were digitized to locate the principal point. The 1936 photographs, however, have only one fiducial mark (reseau) in the center of each image to identify the principal point. The marks around the perimeter were cropped off during production of the prints. An attempt was made to locate the original negatives so that new photos could be printed, but many of the negatives had been inadvertently destroyed in storage. (This situation highlights some of the problems encountered when using older photography.)

After digitizing the fiducials, the ground control and pass points on each photo were digitized in point mode. The shoreline was digitized using a 5 pts/sec track mode. The wet/dry line on the beach was used to delineate the shoreline in each photo.

The DSMS program *images* was used to convert the photo coordinates (in digitizer units) to image space coordinates centered on the principal point. *Images* also formats the image data into separate files for use in the space resection and aerotriangulation programs. Other DSMS programs were used to input additional data for each photograph, such as the lens focal length of each camera used.

Images employs a preprocessing algorithm to remove film deformation from digitized data, if camera system calibration data are available. For the 1987 photographs, calibration data that furnish the location of the fiducial marks inside the camera system were used to remove film deformation effects using four fiducial mark locations and a first degree polynomial transformation.

Calibration data were unavailable for the 1936 and 1951 photos, so the fiducial coordinates were estimated using their respective camera formats (229 × 185 mm; 229 × 229 mm) as well as general information provided by the organizations that performed the aerial surveys. While not quantitatively removing film deformation, this approach does have the advantage of reducing all photos taken with the same camera system to a common image space system. When used in this manner, a first degree polynomial transformation removes much of the gross error that occurs during the independent digitizing of the fiducial coordinate system on multiple photos by mapping the digitized coordinates for each photo in a given set to a common image space system. The residual errors from the transformation also provide a means to assess the accuracy and consistency of the person digitizing the photos.

An initial space resection, using the DSMS program *frames*, was performed for selected photographs to provide a first approximation of the camera parameters and residual errors for various ground control points. The *GIANT* aerotriangulation program was used to solve simultaneously for the camera parameters for a small group of nine photos covering the Punta Uvero area. *GIANT* was also used to remove atmospheric refraction effects from the aerotriangulation solution.

The camera parameters for each photo determined by *GIANT* were used to compute a single-ray intersection solution for the digitized shoreline points using the DSMS program *shoreline*. A geographic coordinate system based on the Clarke 1866 ellipsoid was used in shoreline position calculations. These coordinates were converted to UTM values for import into the Punta Uvero GIS file. The elevation of the wet/dry line defined in *shoreline* was 0.3 m. This elevation was determined based on general tide information, field visits, and examination of each set of photographs to evaluate wave height and swash runup characteristics, which could have affected the horizontal position (elevation on the beach) of the wet/dry line on the date of photography.

The output shoreline position data files for each photo were imported into separate overlays (one for each year of photography) in the MapGrafix GIS file, and joined to adjacent photo data to form a continuous shoreline. In the GIS file, a measurement baseline was established landward of the shorelines by drawing an open polygon parallel to the general shoreline trend. The shoreline and baseline data were exported from the GIS as an ASCII text file for use in the DSAS. The DSAS programs *transect* and *rates* were used to calculate shoreline rates-of-change at 100 m intervals along the baseline.

RESULTS

A shoreline change map for Punta Uvero, including both the map and photograph data, is shown in Figure 8. The important result of a mapping exercise, however, is not necessarily a map, but the accuracy of the shoreline data shown on the map, since their positional accuracy defines the map's accuracy, which affects any subsequent analyses such as shoreline rate-of-change calcu-


8 1936
K-15-


GS-LR-12
FEB 4 1951

Figure 6. Three photos used in the Punta Uvero data set show the different types of imagery used in this study. The shoreline indicator used in this study is the wet/dry line, which is identifiable in each photo by the tonal difference between wet and dry beach sand. Note the dramatic change in the morphology of the point since 1936. (Top, A) This 1936 black-and-white air photo of Punta Uvero has a scale of about 1:18,000. The photo failed to achieve a stable space resection solution and was excluded from the analysis. (Bottom, B) A 1951 black-and-white photograph of Punta Uvero. The scale is approximately 1:15,000. (Above, C) A 1987 natural color photograph of Punta Uvero. The scale is approximately 1:20,000.

lations. Thus, it is crucial that the accuracy of the shoreline position data be quantified so that the quality of subsequent data analyses can be assessed. There are several methods available that permit map and photo errors to be quantified, such as examining the errors in the data reduction process.

Map Transformations

Errors in the map data are reflected in the residual errors from the digitizer-to-geographic coordinate transformation process. The NOS T-sheets, for example, were converted from digitizer to geographic coordinates using eight calibration points and a first degree polynomial transformation. The points are displaced by an average of 0.16 mm, which translates to an error of 1.6 m at the 1:10,000 scale of the map (Table 2). These measurements are within the limits imposed by the resolution of the digitizing table (0.025 mm) and the digitizer operator (0.2 mm). Similar errors are described by CROWELL *et al.* (1991) for T-sheets of the U.S. East Coast published after 1954.

For ground control points obtained from the USGS map, a first degree transformation using 12 calibration points was employed. The average error for the 12 points is 0.125 mm, which at the 1:20,000 scale of the map is an error of 2.5 m (Table 3). Repeated digitizing of geodetic control and other well-defined prints for which a field-surveyed position is available showed that both of the maps used in this example are within the prescribed National Map Accuracy Standards (0.508 mm) for maps at a scale of 1:20,000 or larger (THOMPSON, 1987).

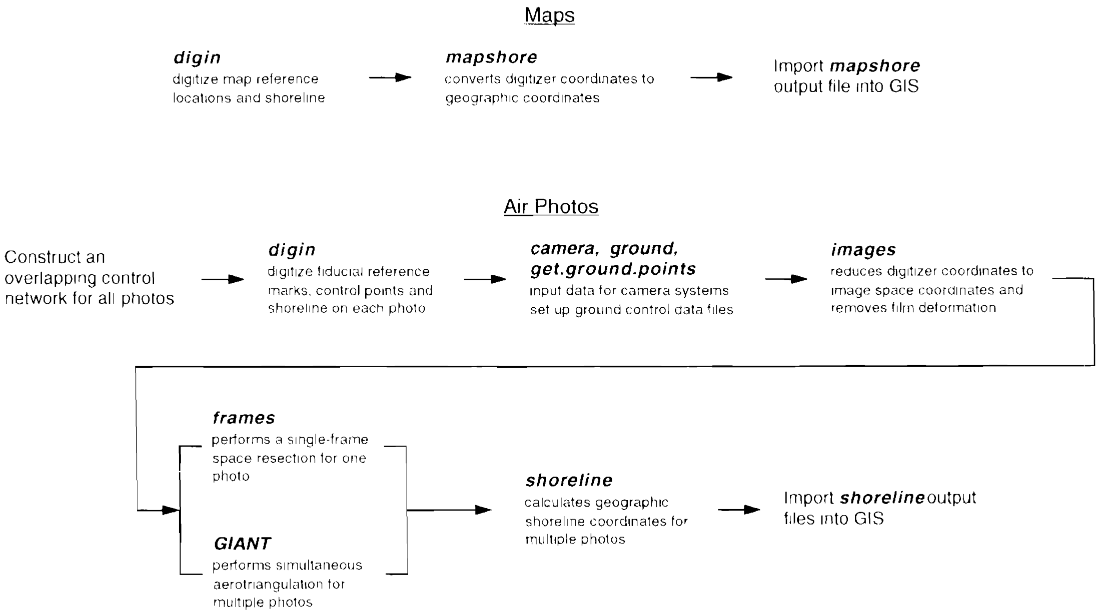

Figure 7. Flow diagram of the basic steps in DSMS execution to obtain shoreline position data from maps and aerial photographs. Specific program names are shown in italics.

Photo Transformations

A number of errors are introduced during the data reduction process for aerial photographs. These errors include those made in digitizing the photos, as well as in aerotriangulation adjustments that incorporate other sources of error such as inaccurate ground control locations. Thus, two measures of error exist for air photos: (1) measurement or digitizer error, and (2) aerotriangulation errors. The *GIANT* aerotriangulation program, however, provides the capability to include both sources of error when formulating an error assessment for a given group of photographs.

Measurements made on the photos have a standard deviation of 0.038 mm. This value was determined by repeated digitizing of points in several different sets of photos and examining the residual pointing error of the digitizer operator. The *images* preprocessing program was also used to examine the residual errors from the reduction of photos from the same set to a common image space system, and provided a further check on the accuracy and consistency of the operator.

Table 4 shows the results of the initial space resection solution for the photos from the Punta Uvero data set shown in Figure 6A, 6B and 6C. The 1936 photo failed to achieve a stable solution after 10 iterations of the initial space resection program. Redigitizing, checking of control points, and estimation of camera parameters in *GIANT* using synthetic data were unable to resolve this problem, so the photo was discarded. In the aerotriangulation adjustment performed by *GIANT*, the 1936 photos consistently caused the solution to become unstable. As a result, the photos were discarded. The *GIANT* program was then re-run using only nine photos, four from 1951 and five from 1987. This group achieved acceptable solutions and residuals.

Four forms of *GIANT* output are useful for assessing errors in digitizing, aerotriangulation, and subsequent shoreline location calculations: (1) the estimated variance of unit weight for the entire group of photos, (2)residual errors for digitized image coordinates, (3) adjustments applied to ground control, and (4) triangulated camera parameters. The volume of output from a *GIANT* run is quite large for a even a small number of photos; the relevant results are summarized in Tables 5 and 6.

The *a posteriori* estimate of the variance of unit weight for the nine-photo block is 1.86 (Table 5). The variance of unit weight should approach 1.0, and is calculated based on the input weight assignments for photo and ground control data. The

Table 2. *Residual errors for NOS shoreline map T-12136 (Punta Uvero) using 8 calibration points and a first degree polynomial transformation.*

Map Longitude	Map Latitude	Digitized Longitude	Digitized Latitude	Longitude Residuals (m)	Latitude Residuals (m)	Total Offset (m)
65°52′30″W	18°27′15″N	65°52′29.967″W	18°27′15.058″N	-0.98	-1.79	2.03
65°52′30″W	18°25′00″N	65°52′30.036″W	18°24′59.997″N	1.05	0.10	1.05
65°52′30″W	18°22′30″N	65°52′30.028″W	18°22′29.929″N	0.82	2.18	2.33
65°50′30″W	18°22′30″N	65°50′29.953″W	18°22′30.020″N	-1.38	-0.63	1.51
65°48′45″W	18°22′30″N	65°48′44.989″W	18°22′30.041″N	-0.33	-1.25	1.31
65°48′45″W	18°25′00″N	65°48′45.027″W	18°25′00.024″N	0.81	-0.73	1.08
65°48′45″W	18°27′15″N	65°48′45.019″W	18°27′14.917″N	0.55	2.55	2.61
65°50′30″W	18°27′15″N	65°50′29.982″W	18°27′15.014″N	-0.55	0.43	0.68
						Avg. 1.58

Note: Map scale = 1:10,000.

observed value indicates that the weight assignments for each component are reasonable, given the quality of the ground control and photo measurements.

When multiplied by the assumed input standard deviation (0.038 mm) for photo measurements, the standard deviation of unit weight (1.36; Table 5) provides a basis for assessing the computed standard deviation of image points. Using this technique, the root mean square (RMS) error for points digitized on the photos computes to 0.052 mm, which corresponds to about 1.0 m on the ground at photo scale.

The RMS error for computed positions of ground control points is 8.5 m in longitude, 10 m in latitude, and 0.3 m in elevation (Table 5). These adjustments are made by *GIANT* to fit the image points to the ground control, and are within the specified National Map Accuracy Standards for the USGS map used to obtain the ground control data.

Table 6 shows the triangulated camera stations for the photos in the Punta Uvero group. The computed stations agree with known values for flight height and flight line characteristics.

Shoreline Rates-of-Change

The measurement baseline and shore-perpendicular transect locations used to determine shoreline rates-of-change for Punta Uvero are shown in Figure 9. Table 7 shows the rates of shoreline change calculated by the methods used in the DSAS. The end-point rates are plotted in Figure 10. Erosion is clearly the dominant shoreline trend. Only two transects, west of Punta Uvero, show accretion over the 36 year period 1951–1987.

DISCUSSION

There are five types of errors inherent inshoreline mapping that affect the accuracy of shoreline positions obtained from maps and photos: (1) inaccurate source data, (2) careless mistakes or blunders, (3) constant errors (*e.g.*, measuring instrument), (4) systematic errors (*e.g.*, lens distortion), and (5) random errors (*e.g.*, operator). The amount of error in maps and surveys used as a source of ground control or shoreline data depends upon both their accuracy (field surveys) and scale (if digitized from a map). Careful screening of the data, however, can keep these errors within acceptable limits. Blunders are (hopefully) corrected in the early stages of data processing. Both constant and systematic errors can be removed or minimized in preprocessing. Random errors, such as those made during digitizing, are generally considered to be normally distributed around zero; their magnitude can be quantified by testing the repeatability of measurements on maps and photos made by a given person.

We assume the shorelines shown in Figure 8 represent an average seasonal shoreline position. Both sets of photography, for example, were flown during the winter season; the field surveys for the T-sheets were also performed in the winter. Historical meteorological, wave and water level data were checked for events that may have affected the shoreline position on the photography and field survey dates, but the data are inconclusive. This is largely because the north coast of Puerto Rico receives much of its winter wave energy from storms in the North Atlantic, and few data are available on their local effects (*e.g.*, FIELDS and JORDAN, 1972). A check was conducted for the survey dates of each T-sheet with the same result.

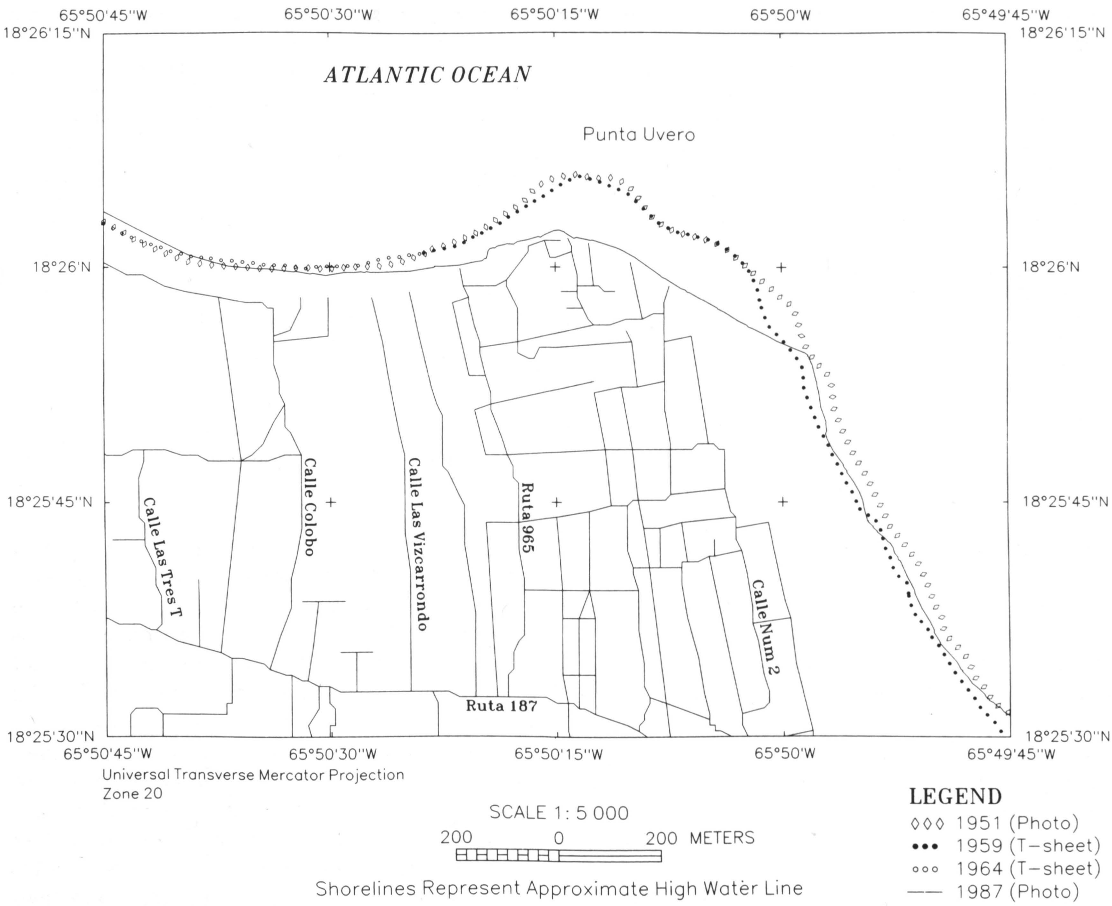

Figure 8. The shoreline change map for Punta Uvero includes both map and air photo data. The roads shown here were obtained from digital TIGER/Line data (U.S. BUREAU OF THE CENSUS, 1991).

The photos were also examined to assess the wave energy on the date of photography, which might have artificially displaced the wet/dry line from its "average" location. Wave energy in the study area is low and about equal for both sets. Thus, it is probably reasonable to assume that the shorelines used in this example are representative of at least a winter shoreline position.

In this discussion, we are primarily concerned with two questions: (1) "How accurate are the locations shown on the map?" and (2) "What is the resolution of rate-of-change measurements made on the map?" It is necessary to distinguish between accuracy and resolution because they have a different value and meaning. Accuracy refers to the degree of perfection attained in placing points on the map relative to their true locations. Resolution refers to the level of uncertainty or "noise" inherent in measurements made on the map. In determining an erosion rate, for example, one is not necessarily concerned with the absolute positions of the shorelines in space, but the accuracy of their positions relative to each other. Both accuracy and resolution can be determined by examining the errors in the source materials and data reduction procedures, and provide insight into the errors contributed by the various source materials and methods used.

Map Transformations

As discussed above, the T-sheet and 7.5-minute topographic maps of Punta Uvero are within National Map Accuracy Standards (NMAS). However, a second degree polynomial transformation could have been used to further reduce the RMS error in the T-sheet data since eight calibration

Table 3. *Residual errors for USGS topographic map Rio Grande, P.R. using 12 calibration points and a first degree polynomial transformation.*

Map Longitude	Map Latitude	Digitized Longitude	Digitized Latitude	Longitude Residuals (m)	Latitude Residuals (m)	Total Offset (m)
65°52′30″W	18°30′00″N	65°52′30.017″W	18°29′59.901″N	0.51	3.05	3.09
65°52′30″W	18°27′30″N	65°52′30.035″W	18°27′30.060″N	1.01	−1.84	2.10
65°52′30″W	18°25′00″N	65°52′30.033″W	18°24′59.904″N	0.98	2.95	3.11
65°52′30″W	18°22′30″N	65°52′29.895″W	18°22′29.963″N	−3.09	1.15	3.29
65°50′00″W	18°22′30″N	65°50′00.046″W	18°22′30.053″N	1.34	−1.64	2.12
65°47′30″W	18°22′30″N	65°47′29.954″W	18°22′30.063″N	−1.34	−1.93	2.35
65°45′00″W	18°22′30″N	65°45′00.087″W	18°22′30.005″N	2.57	−0.16	2.57
65°45′00″W	18°25′00″N	65°44′59.997″W	18°24′59.947″N	−0.09	1.63	1.64
65°45′00″W	18°27′30″N	65°44′59.958″W	18°27′29.987″N	1.22	0.40	1.30
65°45′00″W	18°30′00″N	65°44′59.971″W	18°29′59.927″N	−0.85	2.26	2.41
65°47′30″W	18°30′00″N	65°47′29.998″W	18°30′00.034″N	−0.06	−1.04	1.04
65°50′00″W	18°30′00″N	65°50′00.008″W	18°30′00.157″N	0.25	−4.84	4.85
						Avg. 2.49

Note: Map scale = 1:20,000.

points were digitized and only six are needed to solve second order equations. The improvement in fit (the average offset is reduced from 1.58 m to 0.39 m), however, is less than the thickness of the line representing the shoreline on the map and is well beyond the level of accuracy achieved by the human operator.

It is commonly assumed that map transformation residuals (RMS errors) are representative of the accuracy of a map (*e.g.*, CROWELL *et al.*, 1991). The RMS errors, however, are generally useful only for identifying errors in manually digitizing the map and are not necessarily indicative of its accuracy. For example, the RMS errors shown in Tables 2 and 3 primarily reflect the accuracy of the person who digitized the map, not the map's accuracy. A better measure of map accuracy is obtained by comparing the geographic coordinates of geodetic control points digitized on a map to their field-surveyed locations.

Given the limits imposed by the cartographic representation of points on the USGS map used to determine photograph control point coordinates, as well as the table and operator imposed limits, the residual errors provide an unrealistically low error estimate (2.5 m) to use in the aerotriangulation adjustment. Therefore, the ground control weights (standard deviations of measurement) used in *GIANT* were designed to reflect the potential errors discussed below.

The horizontal basemap error for the USGS map was assumed to be equivalent to NMAS (10.16 m on the ground). The map used in this example, however, appears to exceed these standards. A lower estimate could be justified if field-surveyed positions were available to test specific control points used in the aerotriangulation adjustment.

The combined resolution of the digitizing table and the digitizer operator (0.225 mm) was converted to its ground distance equivalent (4.5 m) at the scale of the USGS topographic map (1: 20,000) used to determine the ground control point coordinates and added to the horizontal basemap error of 10.16 m. Thus, the total horizontal error for a control point may be as large as 14.66 m.

The vertical basemap error in ground control point elevation (determined from the USGS map) was assumed to meet NMAS for elevation (elevations must be correct to within one-half of the contour interval), plus a contour interval-dependent human interpreter error assumed to be one-half the contour interval. For a 1 m contour interval, for example, the interpreter was assumed to be accurate ±0.5 m. This approach permits the total vertical error for a control point to be as large as one contour interval.

Photo Transformations

The DSMS relies primarily on the statistical output from *GIANT* to identify the form and magnitude of errors in air photo mapping. In addition, *GIANT* also provides the capability to test independently one or more sets of photographs to assess the effects of lens distortion, film deformation, ground control and the accuracy of image coordinate measurements on the quality of the aerotriangulation adjustment.

Camera calibration data for the 1987 photos permit film deformation and lens distortion characteristics to be quantified and removed. To de-

Table 4. *Output camera parameters from the initial DSMS space resection program for the photos shown in Figure 6A–C: photo identification, iteration results and residuals.*

(1936) Photo No. k15-1425

Camera	X	Y	Z	Roll	Pitch	Yaw
INIT	199,780.73	2,038,586.88	229.77	0 0 0	0 0 0	4 16 4
ITER 1	200,155.58	2,039,394.12	5,835.14	0 2 55	1 20 49	−4 24 15
ITER 2	200,302.61	2,039,474.59	5,806.84	0 47 59	1 28 26	−4 24 39
ITER 3	200,310.86	2,039,498.44	5,799.77	−1 2 17	1 33 5	−4 25 3
ITER 4	200,313.75	2,039,507.90	5,797.29	1 7 55	1 34 43	4 25 11
ITER 5	200,314.85	2,039,511.40	5,796.38	−1 9 59	1 35 20	−4 25 14
ITER 6	200,315.25	2,039,512.71	5,796.05	−1 10 46	1 35 34	−4 25 16
ITER 7	200,315.40	2,039,513.20	5,795.92	1 11 3	1 35 39	−4 25 16
ITER 8	200,315.46	2,039,513.38	5,795.88	1 11 10	1 35 41	4 25 16
ITER 9	200,315.48	2,039,513.44	5,795.86	1 11 12	1 35 42	−4 25 16
ITER 10	200,315.49	2,039,513.47	5,795.85	1 11 13	1 35 42	−4 25 16

********SOLUTION FAILS TO CONVERGE********

(1951) Photo No. 1r12-92

Camera	X	Y	Z	Roll	Pitch	Yaw
INIT	199,079.70	2,038,696.88	94.53	0 0 0	0 0 0	2 41 48
ITER 1	199,313.64	2,039,123.28	2,400.48	2 23 6	−0 36 49	−2 43 59
ITER 2	199,294.79	2,039,207.86	2,384.84	−2 7 38	0 29 15	2 45 6
ITER 3	199,294.09	2,039,209.33	2,385.01	−2 9 38	−0 30 14	−2 45 8
ITER 4	199,294.18	2,039,209.15	2,385.04	−2 9 22	−0 30 6	−2 45 8
ITER 5	199,294.17	2,039,209.17	2,385.04	2 9 24	−0 30 7	−2 45 8
ITER 6	199,294.17	2,039,209.17	2,385.04	2 9 24	0 30 7	2 45 8

Point	X	Y		VX	VY
23	197,508.70	2,037,914.09	1.00	0.91	−0.97
24	198,206.15	2,038,384.00	1.50	−4.49	−1.27
25	198,685.00	2,038,884.42	2.00	−11.45	13.81
26	198,883.57	2,038,103.18	1.00	19.56	−1.16
27	200,152.98	2,039,517.49	2.00	−8.31	7.36
28	201,041.86	2,039,377.97	2.00	4.63	−3.06

(1987) Photo No. 14-260

Camera	X	Y	Z	Roll	Pitch	Yaw
INIT	199,942.12	2,039,157.75	121.03	0 0 0	0 0 0	1 55 57
ITER 1	200,794.64	2,039,521.52	3,068.88	−1 5 52	0 11 0	−1 48 10
ITER 2	200,803.68	2,039,580.36	3,058.15	1 6 27	0 11 31	−1 47 58
ITER 3	200,803.67	2,039,580.37	3,058.14	−1 6 27	0 11 31	−1 47 58

Point	X	Y		VX	VY
01	198,771.97	2,040,270.99	3.00	6.13	2.72
03	198,971.43	2,038,273.88	1.00	0.90	8.82
04	198,893.47	2,039,330.61	1.00	−8.64	−1.46
05	199,703.88	2,039,687.40	2.00	−11.14	−10.04
06	200,543.14	2,039,777.10	2.00	12.54	2.83
07	201,353.26	2,039,162.43	1.00	−7.39	2.83
08	201,357.71	2,037,601.56	1.00	7.66	0.22

Notes: The X Y values and residuals are in UTM (meters). Elevations (Z) are in meters above sea level. Camera attitude (roll, pitch, yaw) is in degrees, minutes, and seconds. All of the 1936 photos failed to achieve a solution after 10 iterations. The 1951 and 1987 photos, however, have acceptable parameters. UTM values for the 1951 and 1987 photos were converted to geographic coordinates and input to the *GIANT* aerotriangulation program as part of a small group of nine photos.

Table 5. *Summary of error analysis provided by GIANT for various aerotriangulation parameters.*

Category	Description	Magnitude
Triangulated ground point residuals (weighted sum of squares)	Ground	60.8 μm
	Photos	39.7 μm
	Total	100.4 μm
	d.f.	54
A posteriori estimates for unit weight	Variance	1.86
	Std. dev.	1.36
RMS errors for camera stations (n = 9)	Longitude	0°0′1.3116″
	Latitude	0°0′2.1894″
	Elevation	27.4935 m
	ω (roll)	1°23′16.7178″
	φ (pitch)	0°48′28.4480″
	κ (yaw)	0°21′54.5784″
RMS errors for ground points	Longitude	0°0′0.2939″ (8.8 m)
	Latitude	0°0′0.3225″ (9.7 m)

Table 6. *Triangulated camera stations determined by GIANT for the nine-photo Punta Uvero group.*

Photo	Position		Attitude	
14-260	lng	65 49 55.8866	roll	1 5 24.9100
	lat	18 25 35.0702	pitch	−0 8 53.2894
	elv	3,056.1904	yaw	0 54 44.8383
14-262	lng	65 47 56.3166	roll	0 30 14.4802
	lat	18 25 31.9002	pitch	0 29 40.8056
	elv	3,102.5115	yaw	1 44 20.3066
14-263	lng	65 46 52.2876	roll	0 2 32.9916
	lat	18 25 33.0766	pitch	0 37 40.6584
	elv	3,082.7182	yaw	0 28 9.9471
15-367	lng	−65 48 12.0627	roll	0 16 13.9523
	lat	18 23 39.2916	pitch	0 8 5.3466
	elv	3,209.7416	yaw	0 10 5.5417
15-368	lng	65 47 7.7691	roll	1 26 15.8182
	lat	18 23 41.1603	pitch	0 26 54.9012
	elv	3,193.4774	yaw	−0 46 57.4242
lr12-80	lng	−65 46 5.4351	roll	0 44 57.6220
	lat	18 23 58.4611	pitch	1 55 8.1015
	elv	2,396.4069	yaw	−2 3 19.7098
lr12-86	lng	−65 45 55.8533	roll	−1 13 47.5738
	lat	18 25 17.6760	pitch	0 17 42.0420
	elv	2,405.3420	yaw	1 19 44.8952
lr12-90	lng	65 49 12.4015	roll	0 38 4.9774
	lat	18 25 19.5989	pitch	0 6 32.5786
	elv	2,369.8495	yaw	1 50 13.4752
lr12-92	lng	65 50 47.0465	roll	2 10 21.2239
	lat	18 25 22.3400	pitch	0 35 27.3683
	elv	2,382.0633	yaw	1 50 19.8359

Notes: Each of the photos designated L4-*nnn* and L5-*nnn* are from a single strip (flight line) of photography. L4 and L5 lines of flight are west-east. LR12-86, LR12-90 and LR12-92 are also from a single strip (east-west). Camera positions are in degrees, minutes and seconds. Elevations are in meters above sea level. Camera attitude is in degrees, minutes and seconds.

termine the magnitude of film deformation and also monitor the accuracy of the digitizer operator, the DSMS *images* program calculated residual errors for the calibrated fiducial mark locations and the fiducial system digitized on each photo. The error introduced by film deformation for each photo is generally less than 0.002 mm, but the sense and magnitude of error is not consistent between photos.

The maximum lens distortion in the camera system used for the 1987 photography is approximately 0.004 mm, according to a calibration report produced for the camera system just prior to the date of photography. This amount of lens distortion introduces a negligible error on the ground (a few centimeters) at the scale of the photos.

As discussed above, the digitized 1936 and 1951 photo data were not preprocessed to remove film deformation or lens distortion because calibration data were unavailable. Thus, potential errors include operator error as well as errors introduced by film deformation and lens distortion. Film deformation, for example, affects all for the data measured on a photograph by changing the spatial relationship between the fiducial marks used to define the image space coordinate system and to calculate the location of points in the photo. It is likely, however, that using the estimated fiducial coordinate locations removed any significant film deformation present in these photos.

Lens distortion adds to the potential error in image coordinate locations by further displacing the points from their true positions. For example, the lens distortion present in the 1936 photos is of sufficient magnitude to make space resection solutions unstable using either a limited single-frame space resection solution that holds image and ground point values constant or a more flexible solution in which the input parameters can be varied. To identify the source of the instabilities in the aerotriangulation adjustment, several tests were conducted in which different combinations of synthetic camera parameters and measurement weights were submitted to *GIANT*. In each case, the aerotriangulation solution became unstable. In addition, none of the photos have a significant amount of film deformation (the photos average about 0.05 mm) that could cause the same problem.

An important lesson derived from this situation

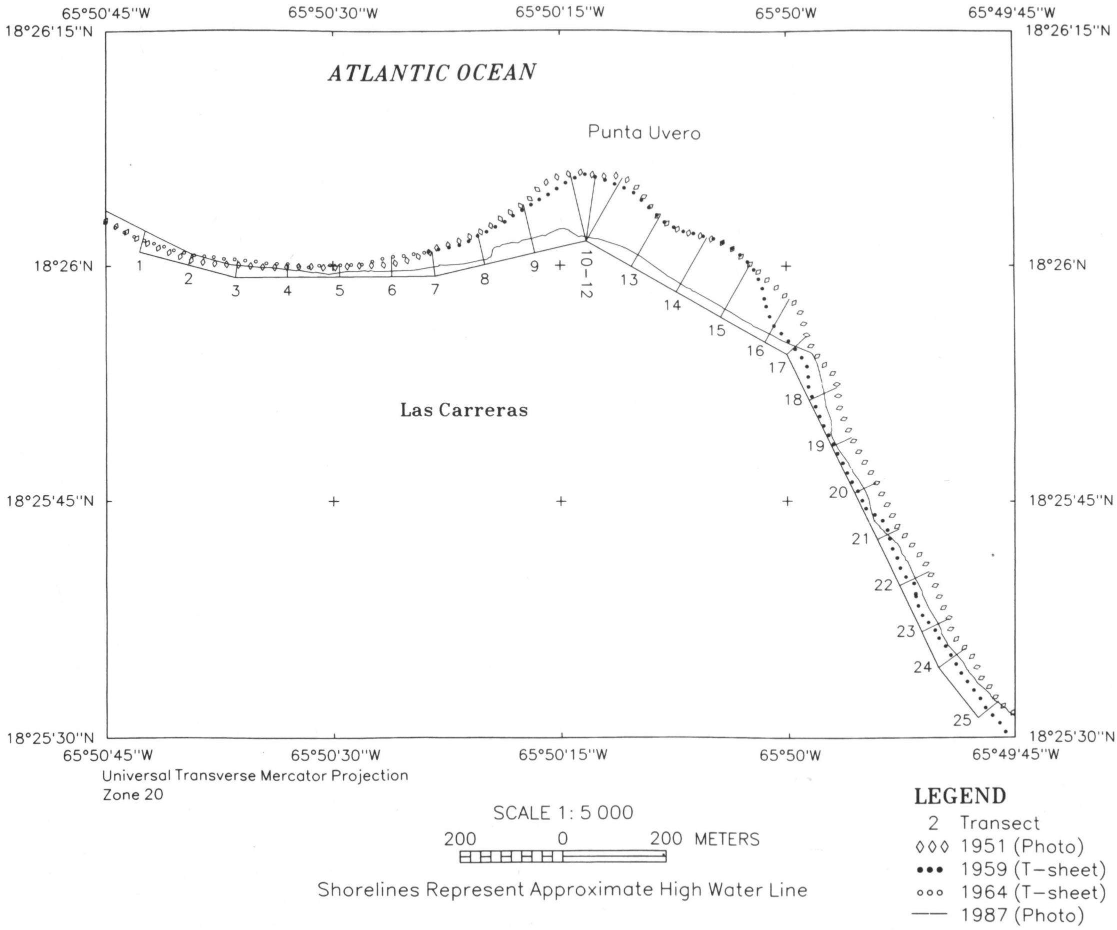

Figure 9. A measurement baseline was established parallel to the general shoreline trend to determine the rate of shoreline change along transects drawn orthogonal to the baseline at 100 m intervals. An open polygon drawing tool was used in the GIS to manually draw the baseline. Where the baseline changes orientation, the DSAS algorithm establishes a transect at the baseline vertex so that a data gap is not created (*e.g.*, Transect 11). The location of shoreline positions along a transect is determined by the intersection of the transect line with each shoreline. The seawall shown in Figures 2 and 3 is visible as the seaward bulge in the 1987 shoreline (solid line) between transects 8 and 10.

is that the DSMS can resolve imperfections in aerial photography that commonly are assumed to be nonexistent. Other techniques for obtaining shoreline positions from air photos typically are not able to detect such errors. The potential errors introduced by including bad data are often sufficiently large to alter completely the quantified history of shoreline changes. This is particularly true for the oldest data point, which forms the basis for a number of shoreline rate-of-change calculations (Dolan *et al.*, 1991).

How "Real" are the Shoreline Changes at Punta Uvero?

The map in Figure 8 shows the shoreline position at various moments in time, and provides a basis for quantifying such parameters as a rate of shoreline change, or changes in shoreline orientation over time. The accuracy of the map, however, limits the quality of the measurements made from it. A truly rigorous discussion of accuracy requires statistical analysis beyond the scope of

Table 7. *Shoreline change rates for Punta Uvero, P.R. calculated by the DSAS.*

Transect	epr (m/yr)	aor (m/yr)	σ aor	s aor	lr (m/yr)	jk (m/yr)
1	0.58	0.69	0.11	0.01	0.61	0.53
2	0.34	0.34	0	0	0.31	0.42
3	−0.02	*	*	*	0.07	0.1
4	0.14	*	*	*	0.18	0.05
5	−0.31	*	*	*	0.35	0.21
6	−0.38	0.38	0	0	0.48	0.17
7	−0.84	0.96	0.13	0.02	0.9	0.63
8	1.49	−1.27	0.5	0.25	1.56	1.27
9	−1.92	−1.71	0.48	0.23	1.98	1.71
10	−3.52	3.04	1.12	1.26	3.67	3.04
11	−3.4	2.69	1.66	2.74	3.62	2.69
12	3.74	3.32	0.97	0.94	3.87	3.32
13	−2.34	1.8	1.28	1.64	2.52	1.8
14	−2.91	2.21	1.65	2.72	3.14	2.21
15	−2.81	2.21	1.41	1.99	3	2.21
16	−2.2	3.45	2.93	8.58	1.8	3.45
17	0.82	−0.33	0.49	0.24	0.57	1.61
18	−0.76	0.04	0.8	0.65	0.35	2.06
19	−0.93	0.4	0.54	0.29	0.66	1.79
20	0.74	−0.14	0.59	0.35	0.43	1.69
21	−0.7	0.41	0.29	0.08	0.55	1.16
22	−0.84	0.24	0.61	0.37	0.53	1.82
23	−0.66	−0.1	0.56	0.31	0.37	1.56
24	−0.58	0.11	0.46	0.22	0.34	1.33
25	−0.07	*	*	*	0.18	0.84

Notes: Negative rate values indicate erosion. A graph of the end-point rate is shown in Figure 10. Dolan *et al.* (1991) provide a complete discussion of the utility of each rate calculation. (epr = end-point rate; aor = average of rates; σ aor = standard deviation of average of rates; s aor = variance of average of rates; lr = linear regression rate; jk = jackknife rate; * data fail to meet the minimum change required to use this method.)

this paper. There are, however, several fundamental parameters that can be used to quantify the various sources of error and obtain an estimate of the accuracy of the map shown in Figure 8. In addition, the maximum error can be used to derive a signal to noise (S/N) ratio that specifies the minimum rate of shoreline change per year above which rates can be considered detectable.

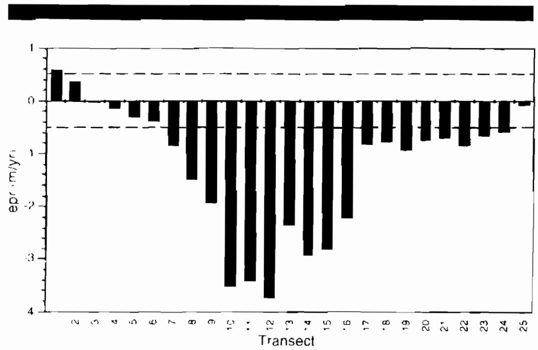

Figure 10. The end point shoreline change rates for Punta Uvero clearly show the erosion dominated shoreline trend. Negative values indicate erosion. The 0.51 m/yr S/N limits are shown by the dashed lines. Rates that fall within the S/N limits are below the resolution of the data and cannot be considered detectable. The transects measured at Punta Uvero are shown in Figure 9.

Since all the potential sources of error in shoreline coordinate calculations are included in the *GIANT* adjustment, an error estimate can be derived from the program's output and applied to the rate of change along the shoreline. The error estimate calculated during the *GIANT* aerotriangulation reflects the uncertainty associated with all error from all sources. For computing errors in shoreline positions and rates-of-change, this is a significant advantage over the "single frame at a time" approach used in some mapping systems (*e.g.*, CLOW and LEATHERMAN, 1984) because all the data are simultaneously registered to a common set of control; a best-fit solution is achieved that identifies and distributes errors and has a unique, quantifiable value.

The covariance matrices determined by *GIANT* for each camera station can also be used to propagate the error in each camera station back to the ground in the single-ray intersection so-

Table 8. *Accuracy of the shorelines mapped from air photos and the resolution of the erosion rates based on errors in the relative locations of the digitized shorelines.*

Category	Description	Magnitude
Observed accuracy of the map shown in Figure 8	Horizontal RMS error for ground coordinates	9.25 m
	Vertical RMS error for ground coordinates	0.3 m
Resolution of end-point rates	Error in oldest shoreline position	9.25 m
	Error in most recent shoreline position	9.25 m
	Total	18.50 m
	Years elapsed between photos	36 yr
	S/N ratio	0.51 m/yr

Note: The map is assumed to comply with National Map Accuracy Standards for a scale of 1:20,000 or larger (10.16 m on the ground), but was not tested.

lution (THIELER and DANFORTH, 1994, this volume). This method provides an important means by which horizontal and vertical errors in shoreline positions can be identified on a point-by-point or photo-by-photo basis. We are presently incorporating this feature into the DSMS.

The geographic adjustment data provided by *GIANT* shows that the horizontal geographic position of the aerotriangulated ground points may have an error of up to 9.25 m (Table 5). Since the digitized image residuals are fairly low, this value primarily reflects the precision of the least accurate data used: manually digitized ground control points from the USGS map. The vertical error (0.3 m) is negligible. It is well within the range of both normal swash excursion differences on the beach and human interpreter error. As discussed below, however, other sources of vertical error are important when digitizing shoreline features that have a highly variable alongshore elevation.

To compute the S/N ratio (Table 8) for rate-of-change calculations, the horizontal error for a second shoreline must be included. When the uncertainty in the position of the second shoreline (9.25 m) is added, the total possible error in the shoreline positions is 18.5 m. If independent observations are assumed, the probability of an error of this magnitude is only about eight percent, and about half the shoreline positions will be in error by only 9.25 m. For simplicity in rate evaluation, however, the more conservative estimate (18.5 m) is used here.

The total error for two shorelines, divided by the number of years elapsed between the first and most recent shoreline (36 years) yields a S/N ratio of 0.51 m/yr for all end-point rates determined using the 1951 and 1987 shorelines. When applied to the rates in this example (Table 7), six end-point rates do not exceed the S/N ratio of 0.51 m/yr and cannot be considered detectable. A similar method for determining the validity of rates is furnished by DOLAN *et al.* (1980). The average-of-rates method (FOSTER and SAVAGE, 1989; Table 7, this paper) also provides a basis for determining threshold values, and includes the lower error (1.58 m; Table 2) in rate calculations associated with the T-sheet shoreline.

Practical Limitations and Operational Difficulties

From a technical standpoint, historical shoreline mapping is typically performed under rather unfavorable conditions. Hence, there are a number of practical limitations that determine the ultimate accuracy of shoreline data generated using the DSMS. The most common limitations include: (1) poor quality and/or limited ground control; (2) the aerial surveys were not performed for the purpose of shoreline mapping; and (3) insufficient calibration data. These circumstances are particularly true for older photography.

The shoreline position data presented in this paper are affected by all of these limitations. For example, the most important factor limiting the accuracy of the computed shoreline positions is the ground control data. As discussed above, the error in digitizing the aerial photographs is 0.052 mm, or about one meter on the ground. The ground control points obtained from the USGS map, however, are only accurate to ±14.66 m. This attribute significantly degrades the quality of the aerotriangulation solution because it requires that fairly large corrections be made to fit the photos to the control. As shown in Table 5, the combination of points used in this example have an average horizontal error of about 9.25 m.

Horizontal errors in the shoreline position are also introduced when a shoreline indicator such as a cliff or bluff edge is digitized that has a highly variable alongshore elevation (approximately 3–5 m or more). Since image points are offset horizontally from their true positions due to relief displacement in the photographic image, simple tracing of a variable-elevation cliff edge on a photograph results in a set of image coordinates that are not corrected for relief displacement. Thus, the elevation used in the single-ray intersection introduces a horizontal error that increases with increasing distance between the actual and assumed elevation of the shoreline indicator. As discussed above, however, this is not a significant problem for the Punta Uvero data, since the wet/dry line on the sandy beach was used to delineate the shoreline.

The flight patterns for all three sets of photographs were not optimized for shoreline mapping. The most important implication of this situation is that many photographs which show the shoreline also contain a substantial portion of ocean (*e.g.*, Figures 6A and 6C). This results in a landward bias in the control network that "pulls" the camera station solutions away from their true values (*e.g.*, excessive roll may be introduced). This problem can often be overcome by digitizing several points on the water surface so that the points are sufficient in number and distribution to provide balanced control for the photograph. Using an estimated water level (*e.g.*, 0.1 m), such points can be specified in the *GIANT* program as control points having only a vertical component. This approach often provides the additional control required to use photos that show only a small land area or have control or pass points concentrated in one part of the scene.

The lack of lens distortion data for the 1936 and 1951 photographs also affects the shoreline positions and rate-of-change calculations. In the case of the 1936 photos, the distortion could not be removed and is so severe that the photos could not be used. Assuming the same horizontal error for shoreline points shown in Table 8, the temporal span gained by including the 1936 photos (the record is extended from 36 to 51 years) increases the resolution of the calculated shoreline rates-of-change by 30 percent, from 0.51 m/yr to 0.36 m/yr.

CONCLUSIONS

The Digital Shoreline Mapping System (DSMS) represents a significant step toward the standardization and rigorous application of photogrammetric and cartographic techniques in coastal mapping. The DSMS provides a means to quantify and analyze sources of error, and can be easily modified to meet the needs of almost any project. The DSMS and the DSAS can be used with a variety of source materials and imposes a reasonably low hardware, software and computational overhead. In addition, the entire shoreline mapping process can be rapidly and easily executed by a single person in a small lab. These attributes permit its application to a wide range of coastal mapping problems in a variety of laboratory settings.

The example of DSMS application presented here has several implications for shoreline mapping (1) it is possible to identify accurately, and in many cases significantly reduce, the form and magnitude of errors in shoreline positions obtained from maps and air photos; (2) errors such as film deformation and lens distortion that are routinely (and often incorrectly) assumed to be unimportant can be easily identified and quantitatively removed; and (3) acceptable levels of accuracy and resolution an be achieved with only marginal-quality source materials if proper data reduction strategies are employed.

ACKNOWLEDGEMENTS

The DSMS/DSAS development project was supported by the U.S. Geological Survey, Branch of Atlantic Marine Geology in Woods Hole, Massachusetts. William C. Schwab, Rafael W. Rodriguez, and Bruce R. Richmond of the USGS rendered invaluable assistance in both the office and the field. Gerald I. Evenden of the USGS provided many valuable suggestions during program development, and through his earlier work, much of the computational foundation upon which the cartographic aspects of the DSMS are built.

Atef A. Elassal and James R. Lucas of the National Ocean Service provided source code for *GIANT* and FORTRAN subroutines (later recoded in C) for single-ray intersection. Randle W. Olsen of the USGS wrote the original version of the DSMS single-frame space resection program. Orrin H. Pilkey and David M. Bush of Duke University provided additional support for one of the authors (ERT) during this project. Amber Taylor drafted the figures. Technical reviews by Bob Morton, Robert Dolan and Michael Fenster improved the clarity and content of the paper. The DSMS/DSAS software and the data summarized in this paper are available upon request to the authors.

LITERATURE CITED

CLOW, J.B. and LEATHERMAN, S.P., 1984. Metric mapping: An automated technique of shoreline mapping. *Proceedings, 44th American Congress on Surveying and Mapping.* Falls Church, Virginia: American Society of Photogrammetry, pp. 309–318.

CROWELL, M.; LEATHERMAN, S.P., and BUCKLEY, M. K., 1991. Historical shoreline change: Error analysis and mapping accuracy. *Journal of Coastal Research*, 7(3), 839–852.

DANFORTH, W.W. and THIELER, E.R., 1992a. *Digital Shoreline Analysis System (DSAS) User's Guide, Version 1.0.* Reston, Virginia: U.S. Geological Survey Open-File Report No. 92-355, 42p.

DANFORTH, W.W. and THIELER, E.R., 1992b. *Digital Shoreline Mapping System (DSMS) User's Guide, Version 1.0.* Reston, Virginia: U.S. Geological Survey Open-File Report No. 92-240, 33p.

DOLAN, R.; FENSTER, M.S., and HOLME, S.J., 1991. Temporal analysis of shoreline recession and accretion. *Journal of Coastal Research*, 7(3), 723–744.

DOLAN, R.; HAYDEN, B.P.; MAY, P., and MAY, S., 1980. The reliability of shoreline change measurements from aerial photographs. *Shore and Beach*, 48(4), 22–29.

ELASSAL, A.A., and MALHOTRA, R.C., 1987. *General Integrated Analytical Triangulation Program (GIANT) User's Guide.* Rockville, Maryland: National Oceanic and Atmospheric Administration Technical Report NOS 126 CGS 11, 66p.

EVENDEN, G.I., 1990. *Cartographic Projection Procedures for the Unix Environment—A User's Manual.* Woods Hole, Massachusetts: U.S. Geological Survey Open-File Report No. 90-284, 63p.

EVENDEN, G.I., 1991. *Notes on a Method to Transform Digitized Coordinates to Geographic Coordinates.*

Woods Hole, Massachusetts: U.S. Geological Survey Open-File Report No. 91-17, 5p.

EVENDEN, G.I. and BOTBOL, J.M., 1985. *User's Manual for Mapgen (Unix version): A Method to Transform Digital Cartographic Data to a Map.* Reston, Virginia: U.S. Geological Survey Open-File Report No. 86-706, 134p.

FIELDS, F.K. and JORDAN, D.G., 1972. *Storm-wave Swash along the North Coast of Puerto Rico.* Washington: U.S. Geological Survey Hydrologic Investigations Atlas HA-430, 2 sheets.

FOSTER, E.R. and SAVAGE, R.J., 1989. Methods of historical shoreline analysis. *In:* MAGOON, O.T. (ed.), *Coastal Zone '89,* (New York: ASCE), pp. 4434–4448.

KAYE, C. A., 1959. *Shoreline Features and Quaternary Shoreline Changes, Puerto Rico.* Reston, Virginia: U.S. Geological Survey Professional Paper 317-B, p. 49–140.

THIELER, E. R. and DANFORTH, W.W., 1994. Historical shoreline mapping (I): Improving techniques and reducing positioning errors. *Journal of Coastal Research,* 10(3).

THOMPSON, M.M., 1987. *Maps for America.* Washington: U.S. Geological Survey, 3rd ed., 265p.

U.S. BUREAU OF THE CENSUS, 1991. *TIGER/Line Census Files (Machine-Readable Files of 1990 Census Data).* Washington, D.C.: U.S. Bureau of the Census, Compact Disc—Read-Only Memory, 1 disc.

U.S. DEPARTMENT OF AGRICULTURE, 1981. *Analytical Mapping System (AMS) User's Guide—Volume III—Analytical Triangulation.* Washington: U.S. Forest Service EM-7140-11, 341p.

VELAZCO-DOMINGUEZ, A.T.; WEBB, R.T.; CINTRÓN, G., and MARTINEZ, R. F., 1985. *Sedimentation and Puerto Rican Coral Reefs.* San Juan, P.R.: Department of Natural Resources Technical Publication, CZMP Task 3.7, 85p.